Published in final edited form as:
Neuroscience. 2010 July 14; 168(3): 591–604. doi:10.1016/j.neuroscience.2010.04.027.

Sympathetic sprouting in visual cortex stimulated by cholinergic denervation rescues expression of two forms of long-term depression at layer 2/3 synapses

Portia A McCoy[1] and **Lori L. McMahon**[2,1]

[1]Department of Neurobiology, University of Alabama at Birmingham, Birmingham AL, 35294

[2]Department of Physiology and Biophysics, University of Alabama at Birmingham, Birmingham AL, 35294

Abstract

Cholinergic innervation of hippocampus and cortex is required for some forms of learning and memory. Several reports have shown that activation of muscarinic m1 receptors induces a long-term depression (mLTD) at glutamate synapses in hippocampus and in several areas of cortex, including perirhinal and visual cortices. This plasticity likely contributes to cognitive function dependent upon the cholinergic system. In rodent models, degeneration of hippocampal cholinergic innervation following lesion of the medial septum stimulates sprouting of adrenergic sympathetic axons, originating from the superior cervical ganglia (SCG), into denervated hippocampal subfields. We previously reported that this adrenergic sympathetic sprouting occurs simultaneously with a reappearance of cholinergic fibers in hippocampus and rescue of mLTD at CA3-CA1 synapses. Because cholinergic neurons throughout basal forebrain degenerate in aging and Alzheimer's disease, it is critical to determine if this compensatory sprouting occurs in other regions impacted by cholinergic cell loss. To this end, we investigated whether lesion of the nucleus basalis magnocellularis (NbM) to cholinergically denervate cortex stimulates adrenergic sympathetic sprouting and the accompanying increase in cholinergic innervation. Further, we assessed whether the presence of sprouting positively correlates with the ability of glutamate synapses in acute visual cortex slices to express mLTD and low frequency stimulation induced LTD (LFS LTD), another cholinergic dependent form of plasticity in visual cortex. We found that both mLTD and LFS LTD are absent in animals when NbM lesion is combined with bilateral removal of the SCG to prevent possible compensatory sprouting. In contrast, when the SCG remain intact to permit sprouting in animals with NbM lesion, cholinergic fiber density is increased concurrently with adrenergic sympathetic sprouting, and mLTD and LFS LTD are preserved. Our findings suggest that autonomic compensation for central cholinergic degeneration is not specific to hippocampus, but is a general repair mechanism occurring in other brain regions important for normal cognitive function.

Keywords

ERK; LTD; m1 mAChR; m3 mAChR; sympathetic sprouting

Corresponding Author: Lori L. McMahon, PhD, Associate Professor, Department of Physiology and Biophysics, UAB, 1918 University Blvd, MCLM 964, Birmingham AL, 35294-0005, Office (205) 934-3523, Fax (205) 975-9028, mcmahon@physiology.uab.edu.

Acetylcholine plays an essential role in acquisition and retention of new memories, including those tasks requiring normal visual function (Mayo et al., 1988, Barefoot et al., 2000, 2002, Bentley et al., 2004). Cholinergic innervation to visual cortex originates in nucleus basalis magnocellularis (NbM), a cell population that degenerates in early stages of Alzheimer's disease (AD) and dementia (Davies and Maloney, 1976, Whitehouse et al., 1982). Deficits in spatial working memory and face recognition tasks are hallmarks of AD and have been thought to result from cholinergic system dysfunction (Dunnett and Fibiger, 1993, Nobili and Sannita, 1997, Rizzo et al., 2000). In fact, the degree of cognitive decline is correlated with the degree of cholinergic cell loss (Perry et al., 1978, Bierer et al., 1995). Accordingly, these deficits are mimicked by administration of muscarinic antagonists in healthy adults and are alleviated in AD patients by cholinergic agonists, specifically those targeted at the m1 subtype of the muscarinic receptor (mAChR) (Drachman and Leavitt, 1974, Bodick et al., 1997, Fisher et al., 2000, Clader and Wang, 2005, Fisher, 2008, Caccamo et al., 2009). However, the mechanisms underlying these effects are not fully understood.

Lesion of basal forebrain cholinergic neurons in animal models of cholinergic degeneration results in sprouting of adrenergic sympathetic fibers originating from the superior cervical ganglia (SCG) into denervated regions (Loy and Moore, 1977, Crutcher, 1981, Booze et al., 1993). These fibers normally only innervate blood vessels, but sprout into denervated fields as a consequence of nerve growth factor accumulation that occurs when cholinergic fibers degenerate (Crutcher, 1987, Conner and Varon, 1995, Scalapino et al., 1996). This sprouting can be prevented by bilateral removal of the SCG (Crutcher, 1987).

Our lab has previously discovered in animals with septohippocampal cholinergic denervation that adrenergic sympathetic sprouting stimulates a reinnervation of hippocampal subfields by cholinergic fibers (Scheiderer et al., 2006). While the origin of these cholinergic fibers has yet to be confirmed, sprouting from the SCG is required for their appearance. We previously showed that unilateral removal of the SCG, at a time point when adrenergic sympathetic sprouting is well established, results in the loss of both the adrenergic sympathetic fibers and the cholinergic reinnervation only on the ipsilateral side. This finding suggests the possibility that the SCG is the source of these cholinergic axons (Scheiderer et al., 2006). In this same study, we also found that an m1 mAChR dependent form of LTD (mLTD) at CA3-CA1 synapses could only be induced in slices from cholinergically denervated animals when the SCG remained intact to permit sprouting. However, mLTD was completely absent in slices from animals when septohippocampal lesion was combined with bilateral ganglionectomy to prevent sprouting. Together these data indicate that sympathetic sprouting is compensatory for lost central cholinergic innervation, and this sprouting is capable of preserving synaptic function dependent upon proper functioning of mAChRs.

The goals of the current study were to determine whether the repair mechanism we discovered in hippocampus is a general mechanism occurring in other brain regions negatively impacted by cholinergic denervation. Because cholinergic innervation is required for acquisition and retention of visually dependent learning and memory, and layer 2/3 synapses in visual cortex express mAChR-dependent forms of LTD (Kirkwood et al., 1999, Choi et al., 2005, Origlia et al., 2006, McCoy and McMahon, 2007), we asked if lesion of NbM to cholinergically denervate visual cortex induces adrenergic sympathetic sprouting and the accompanying cholinergic innervation in visual cortex as it does in hippocampus. Further, we determined if cholinergic denervation prevents the ability of layer 2/3 synapses to express mAChR-dependent plasticity, and if so, whether these plasticities are preserved in animals with sympathetic sprouting. Finally, we wanted to determine if “rescued” mLTD requires the same induction mechanisms as mLTD in sham lesioned control animals.

Experimental Procedures

Experiments were conducted in compliance with NIH guidelines, with an approved protocol from the University of Alabama at Birmingham Institutional Animal Care and Use Committee.

NbM lesions and superior cervical ganglionectomy

Adult male Sprague Dawley rats (10-12 weeks old: Jackson Labs) were randomly assigned to four groups: (1) animals without lesions but underwent surgeries; (2) animals with bilateral removal of the SCG and sham NbM lesion [Data obtained from groups 1 and 2 were pooled (sham) as there was no difference in the electrophysiological data or immunohistochemical staining (Supplemental Fig 1A,B)]; (3) animals with NbM lesion and intact SCG to permit sympathetic sprouting (intact ganglia); (4) animals with NbM lesion and bilateral removal of the SCG to prevent sympathetic sprouting (ganglionectomy).

Animals were deeply anesthetized with isoflurane then placed in a stereotaxic apparatus. The skull was exposed, and small holes were drilled to allow access to the basal forebrain (anterior-posterior (AP) −1.4, lateral (L) +/-2.9 to 3.0, ventral (V) −7.5). A bipolar Teflon coated stainless steel electrode was lowered into the NbM, and current (2 mA for 15 s) was passed through the electrode (Harrell et al., 1995, Scheiderer et al., 2006). Sham lesioned animals underwent the same procedure without current application. Superior cervical ganglionectomies were performed via a neck incision to expose the carotid arteries, followed by removal of the ganglia bilaterally. The ganglia were exposed but not removed in sham lesioned animals.

Electrophysiology

All experiments were performed using standard methods (Scheiderer et al., 2006, McCoy and McMahon, 2007). 12-16 week old Sprague-Dawley rats were anesthetized with isoflurane and decapitated. Coronal slices (400 μm) from visual cortex were cut using a vibratome (Leica VT1000S, Germany) in “high sucrose aCSF” (in mM): NaCl 85; KCl 2.5; $MgSO_4$ 4; $CaCl_2$ 0.5; NaH_2PO_4 1.25; $NaHCO_3$ 25; glucose 25; sucrose 75; kynurenic acid 2; ascorbate 0.5. Following a 30 min incubation in the high sucrose aCSF, slices were stored in standard aCSF (in mM): NaCl 119; KCl 2.5; $CaCl_2$ 2.5; $MgSO_4$ 1.3; NaH_2PO_4 1; $NaHCO_3$ 26; glucose 10; kynurenic acid, 2 mM. Slices were transferred to a submersion recording chamber and perfused with oxygenated aCSF at 27-30°C at a flow rate of 3-4 ml/min. Extracellular field potentials in layer 2/3 were recorded with an Axopatch 2B amplifier (Molecular Devices, Sunnyvale CA). A stainless steel bipolar stimulating electrode (FHC, Bowdoinham, ME) was placed in layer 4, and a glass microelectrode filled with 2 M NaCl was placed in layer 2/3 to record extracellular field potentials. The stimulus duration was set at 0.1 ms and the stimulus intensity was adjusted to yield a baseline field postsynaptic potential (fPSP) of 0.4-0.6 mV. Synaptic events were collected at 0.1 Hz. The peak amplitude of the synaptic response was measured and plotted versus time, each point representing the average of 5 consecutive data points. Data were acquired and stored using custom software written in Labview (gift from Richard Mooney, Duke University). Data are presented as mean ± s.e.m. Statistical significance was determined using Student's t test or one-way ANOVA with Tukey's *post hoc* (ANOVA) where appropriate and results were considered significant at $p<0.05$. Only experiments with <5% change in the original baseline were included in the analysis.

After acquisition of a stable baseline of transmission (at least 20 min) mLTD was induced using a 10 min bath application of 50 μM carbachol (CCh) and low frequency stimulation induced LTD (LFS LTD) was induced with 1Hz stimulation for 15 minutes, consistent with previous reports (Dudek and Bear, 1993, Kirkwood et al., 1999, McCoy and McMahon, 2007). Antagonists were bath applied at least 10 min prior to CCh application. The magnitude of the LTD was measured 35 min following induction of the plasticity.

Immunohistochemistry

In some experiments, to directly correlate the density of cholinergic innervation and presence/absence of sympathetic sprouting with the ability of synapses to express LTD, recorded slices and naïve slices from the same animal (38 slices/14 animals) were immediately placed in Bouin's solution for overnight fixation at the conclusion of the electrophysiological recordings. In other cases, animals were transcardially perfused with 4% paraformaldehyde (PFA) in phosphate buffered saline (PBS) and brains were postfixed in 4% PFA overnight (6 slices/3 animals) then sectioned (70 μm) on a vibratome. Slices were washed three times for 30 min in 1× PBS and then blocked in 10% normal donkey serum (NDS) in 0.3% Triton X-100/PBS for 2 h. Primary antibodies were diluted in 10% NDS in 0.3% Triton X-100/PBS [rabbit or mouse anti-tyrosine hydroxylase (TH), 1:400; rabbit anti-p75 neurotrophin receptor (p75NTR), 1:500; goat anti-vesicular acetylcholine transporter (VAChT), 1:1000; goat anti- choline acetyl transferase (ChAT), 1:200; all from Chemicon, Temecula, CA], and incubated overnight at 4° C. Slices were washed three times for 30 min with 1× PBS followed by incubation with fluorescently labeled secondary antibodies diluted in 10% NDS in 0.3% Triton X-100/PBS (donkey anti-rabbit Alexa 594, donkey anti-rabbit Alexa 488, donkey anti-mouse Alexa 594, and donkey anti-goat Alexa 488; all at 1:300; Molecular Probes, Carlsbad, CA) for 2 h at room temperature. After additional washing, slices were mounted on slides with Permafluor (Immunon, Pittsburgh, PA) and examined on an Olympus DSU spinning disc confocal microscope (Center Valley, PA). Red and green channels were scanned sequentially, and 15 μm stacks of images were obtained in the *z*-axis at 0.8 μm/step. A maximum projection was created and used for quantification. VAChT-positive boutons were analyzed using Slidebook (Olympus, Center Valley, PA). At least four consecutive boutons must be observed to be classified as a fragment of axon and analyzed, as done previously (Scheiderer et al., 2006). All fibers meeting this criterion were measured for total length. The entire field of view (1344 × 1024 μm) was analyzed. Data are presented as mean ± s.e.m. Statistical significance was determined using Student's t test or one-way ANOVA with Tukey's *post hoc* (ANOVA) where appropriate and results were considered significant at $p<0.05$. Importantly, immunohistochemical staining of slices from all animal groups (sham lesioned animals and animals with NbM lesion with and without intact SCG) was done simultaneously to control for variability in the staining reaction. In addition, confocal microscope settings were kept consistent between imaging sessions so that the amount of staining could be accurately compared. Both imaging and quantification were performed with the condition blind to the experimenter.

To confirm completeness of the NbM lesion, sections of brain containing the NbM, were fixed overnight in 4% PFA then sectioned (70 μm) on a vibratome in 1× PBS. NbM cholinergic cell bodies were identified using an antibody to choline acetyltransferase (goat anti-choline acetyltransferase (ChAT), 1:300; Chemicon, Temecula, CA) following the protocol described above. Increased staining around the lesion site, or “edge effect” can be seen in our lesion confirmations; however lesions were considered complete when ChAT staining was absent within the cell body region of the NbM (see supplemental figure 1 C,D). Data from animals with incomplete lesions were discarded from further analysis. It should be noted that complete NbM lesions do not correlate with complete absence of VAChT- positive fibers in visual cortex because other cholinergic cell groups outside of NbM send projections to visual cortex (Houser et al., 1983, Eckenstein and Baughman, 1984).

Chemicals

All drugs were made as 1000× stock solutions in water or DMSO and diluted immediately before use. All drugs were obtained from Sigma (St. Louis, MO, USA), except carbachol (CCh) and U0126, which were acquired from Calbiochem (La Jolla, CA, USA).

Results

NbM lesion induces sympathetic sprouting in visual cortex

To determine whether cholinergically denervating visual cortex by NbM lesion induces adrenergic sympathetic sprouting from the superior cervical ganglia (SCG) and the accompanying increase in cholinergic innervation as it does in hippocampus, we labeled adrenergic and cholinergic fibers using anti-tyrosine hydroxylase (anti-TH) and anti-vesicular acetylcholine transporter (anti-VAChT) antibodies, respectively, and imaged the stained tissue using confocal microscopy.

As expected, we observed thick, torturous tyrosine hydroxylase (TH)-positive fibers 2-4 weeks post lesion, characteristic of sympathetic sprouting in other brain regions (Loy and Moore, 1977, Crutcher, 1981, 1987) in slices of visual cortex from animals with NbM lesion with intact SCG to permit potential sympathetic sprouting (compare Figs 1C2 with A2 and B2). These fibers were rarely observed in sham lesioned animals and never in NbM lesioned animals with bilateral removal of the SCG to prevent the possibility of sprouting. Quantification of TH positive staining shows a significant decrease in the number and total TH fiber length in slices from animals with NbM lesion and bilateral ganglionectomy, which is a consequence of lesioning fibers of passage. However, in animals with NbM lesion and intact ganglia, the TH fiber number and length is not significantly different from sham animals (Table 1), due to adrenergic sympathetic sprouting that is occurring in these animals. It can be noticed in images from an animal with NbM lesion and intact ganglia that many of the TH positive fibers are thicker and have a more tortuous morphology compared to the finer, more delicate TH positive fibers (which represent TH positive fibers originating from the locus coeruleus) in slices from animals with either sham lesions or with NbM lesion and bilateral ganglionectomy. As further support for adrenergic sympathetic sprouting in animals with NbM lesion and intact ganglia, we stained a few remaining slices with the low affinity pan neurotrophin receptor, p75 (p75NTR), because this receptor is expressed by sympathetic, but not central, adrenergic fibers (Dechant and Barde, 2002) and has been used previously to identify sympathetic sprouting (Conner and Varon, 1994). The presence of double anti-TH and anti-p75 labeling in a single fiber indicates that these fibers are indeed sympathetic axons. In the few slices (n=5 slices/3 animals) we were able to stain from NbM lesioned animals with intact ganglia, an average of 8.2 +/- 1 double labeled fibers per section were found, which matched previous descriptions of sympathetic sprouting (supplemental figure 2A) (Loy and Moore, 1977, Crutcher, 1981, 1987).

Increased cholinergic innervation accompanies adrenergic sympathetic sprouting

Importantly, correlated with the adrenergic sympathetic sprouting, significantly more VAChT positive fibers were found in slices from animals with NbM lesion with intact ganglia, as well as a significant increase in total fiber length, compared to slices from animals with NbM lesion and bilateral ganglionectomy (Fig.1A-D, Table 2). Clearly, these data indicate that an increased density of cholinergic fibers accompanies adrenergic sympathetic sprouting in visual cortex. However, VAChT-positive staining in both lesion groups was significantly less than in sham lesioned animals (Fig. 1A-D, Table 2), an obvious consequence of the lesioned-induced cholinergic degeneration.

It is important to note that we do not find a complete loss of VAChT positive fibers in visual cortex even though lesion confirmations show complete loss of ChAT positive cell bodies in the NbM (Supplemental Fig.1C,D). In addition to the NbM, there are other sources of cholinergic innervation to visual cortex, including from substantia innominata and globus pallidus, and there are local cholinergic neurons within cortex itself, which are not lesioned in this study (Houser et al., 1983, Eckenstein and Baughman, 1984). Nevertheless, our findings

clearly demonstrate that sprouting from the SCG is required for the increase in VAChT-positive staining observed in animals with NbM lesion, similar to our previous findings in hippocampus following lesion of the medial septum (Scheiderer et al., 2006).

mLTD and LFS LTD are absent in animals with NbM lesion and bilateral ganglionectomy but are present in animals with sympathetic sprouting

We previously reported that lesion of the medial septum to cholinergically denervate hippocampus causes a loss of an m1 muscarinic receptor dependent LTD (mLTD) at CA3-CA1 synapses (Scheiderer et al., 2006). Because cholinergic neurons throughout the basal forebrain degenerate in aging and in neurodegenerative diseases (e.g. AD), determining whether mLTD expression at synapses in visual cortex is lost as a consequence of cholinergic lesioning and rescued/preserved by sympathetic sprouting from the SCG will indicate that this "repair" mechanism is not specific to hippocampus, but is likely a general phenomenon that occurs in all regions impacted by cholinergic degeneration.

Given this, we wanted to determine if mLTD and LFS LTD at layer 2/3 synapses in visual cortex, both of which are dependent on mAChR function (Origlia et al., 2006, McCoy and McMahon, 2007) but see (Choi et al., 2005) are lost in animals with NbM lesion and bilateral ganglionectomy. Furthermore, if this was found to be the case, we wanted to determine whether one or both plasticities can be "rescued" by sympathetic sprouting.

Because our original characterization of the signal transduction mechanisms required for mLTD induction and expression at layer 2/3 synapses in visual cortex was performed in slices from 3-4 week old animals (Kirkwood et al., 1999, McCoy and McMahon, 2007), we first confirmed that mLTD can be induced in adult sham lesioned animals. As expected, we find that bath application of CCh (50 μM) induces a synaptic depression during agonist application and long-term depression (mLTD) during washout in slices from these animals (Fig. 2A3, 80 +/- 1% of baseline fPSP, n=9 slices/ 7 animals, $P<0.001$; paired Student's *t* test). These effects of CCh at synapses in visual cortex are similar to that previously reported in 3-4 week old rats (Kirkwood et al., 1999, McCoy and McMahon, 2007). Note that results from animals undergoing sham NbM lesion with or without ganglionectomy were combined, as there was no difference between the two groups ($p>0.05$; unpaired Student's *t* test), indicating that ganglionectomy alone does not negatively impact the ability of synapses to express mLTD. When we analyzed the paired pulse ratio (PPR), an indirect measure of presynaptic function (Dobrunz and Stevens, 1997), we find that, like in young rats, there is a significant increase in PPR during CCh application (data not shown, 122 +/- 10% of baseline, n=9 slices/ 7 animals, $p<0.01$; paired Student's *t* test). However, unlike our results from young rats, there is a long-term increase in PPR associated with the expression phase of mLTD (data not shown, 112 +/- 8% of baseline PPR, n=9 slices/ 7 animals, $p<0.01$; paired Student's *t* test).

Next, we determined if the presence or absence of mLTD correlates with the presence or absence of adrenergic sympathetic sprouting and the density of cholinergic innervation in NbM lesioned animals. As shown in Fig. 2B2, bath application of CCh to a slice from an animal with NbM lesion and bilateral ganglionectomy was unable to induce mLTD, similar to our finding in hippocampus when cholinergic denervation is combined with bilateral ganglionectomy (Scheiderer et al., 2006). Immunohistochemical staining of another slice from this animal confirms a deficit in cholinergic innervation compared to sham lesioned animals (Fig. 2A1,B1, Table 2). These data are included in the group immunohistochemical analysis of cholinergic fiber density in NbM lesioned animals with bilateral ganglionectomy (Fig. 1 D). This loss of mLTD was observed in an additional 11 animals and the group electrophysiology data are presented in Fig. 2B3 (99 +/- 1% of fPSP baseline, n=18 slices/ 12 animals, $p>0.05$; paired Student's *t* test). Importantly, the magnitude of the synaptic depression during CCh application is unaffected by the NbM lesion and ganglionectomy ($p>0.05$; unpaired Student's

t test), indicating that not all mAChR-dependent mechanisms are affected. When we analyzed the PPR, we found that, similar to sham lesioned animals, there is a significant increase in PPR during CCh application (data not shown, 115 +/- 10% of baseline PPR, n=9 slices/ 7 animals, $p<0.01$; paired Student's *t* test). However, correlated with a lack of mLTD, there is no long lasting increase in PPR after CCh washout (data not shown, 100 +/-5% of baseline PPR, n=9 slices/ 7 animals, $p>0.05$; paired Student's *t* test).

We next tested whether mLTD could be induced normally in slices from animals with NbM lesion but with intact ganglia to permit sympathetic sprouting. As shown in Fig. 2C2, CCh application to a slice from such an animal successfully induces mLTD. Immunohistochemical staining of another slice from this same animal confirms an increase in cholinergic innervation that accompanies adrenergic sympathetic sprouting (Fig. 2C1, Table 2). These data are included in the group immunohistochemical analysis of cholinergic fiber density in NbM lesioned animals with intact ganglia (Fig. 1 D). This rescue of mLTD expression was observed in an additional 8 animals and the group electrophysiological data are presented in Fig. 2C3. Even though the density of cholinergic innervation is significantly decreased in NbM lesioned animals with intact ganglia as compared to sham lesioned animals, the mLTD magnitude is not significantly different between the groups (sham NbM lesion: 80 +/- 1% of baseline fPSP in sham controls, n=9 slices/ 7 animals vs NbM lesion + intact ganglia: 81 +/- 1% of baseline fPSP, n=16 slices/ 9 animals, $p>0.05$; unpaired Student's *t* test). These data indicate that when sympathetic sprouting is permitted, mLTD induction and expression occurs normally. Analysis of the PPR shows a significant increase during CCh application (data not shown, 115 +/- 7% of baseline PPR in lesioned animals with intact ganglia, n=9 slices/ 8 animals, $p<0.01$; paired Student's *t* test), that remains elevated during mLTD expression (data not shown, 112 +/- 6% of baseline PPR in lesioned animals with intact ganglia, n=9 slices/ 8 animals, $p<0.001$; paired Student's *t* test). Thus, when mLTD is successfully induced in either sham lesioned or NbM lesioned animals with intact ganglia, a significant increase in PPR is present during mLTD expression. However, the maintained CCh induced increase in PPR is absent in slices from animals with NbM lesion and bilateral ganglionectomy, which do not express mLTD.

We next wanted to determine if the loss and rescue of mLTD is selective for this plasticity, or if any plasticity that requires mAChRs would be similarly impacted by NbM lesion with and without bilateral ganglionectomy. LTD at layer 2/3 synapses in visual cortex induced by low frequency stimulation (LFS LTD, 1Hz for 15 min) has been shown to be dependent upon mAChR activation and cannot be induced in either single or double m1/m3 knock-out animals (Origlia et al., 2006). We also find that bath application of the mAChR antagonist, atropine (1μM), prevents induction of LFS LTD in control unlesioned animals (1 Hz, 15 min) (Fig 3A2, 93 +/- 4% of baseline fPSP in atropine, n=5 slices/4 animals vs. 73 +/-4% of baseline fPSP in interleaved controls without atropine, n=5 slices/4 animals, $p<0.01$; unpaired Student's *t* test, confirming the requirement of mAChRs in this form of LTD. Therefore, we next tested the impact of NbM lesion with and without intact ganglia on LFS LTD. As shown in Fig. 3C2, LFS LTD is absent in a slice from an animal with NbM lesion and bilateral ganglionectomy (same animal as in Fig. 2B), which correlates with a deficit in cholinergic innervation observed in an immunostained slice from this same animal (Fig. 3C1, same image as in Fig. 2B1; Table 2). These data are included in the group immunohistochemical analysis of cholinergic fiber density in NbM lesioned animals with bilateral ganglionectomy (Fig. 1 D-F). As before, LFS LTD is absent in slices from all animals tested with NbM lesion and bilateral ganglionectomy (Fig. 3C3, 97 +/- 2% of baseline fPSP, n=10 slices/ 7 animals, $p>0.05$; paired Student's *t* test). In contrast, in a slice from an animal with NbM lesion and intact ganglia, LFS LTD is successfully induced (Fig. 3D2). This correlates with an increased density of cholinergic fibers identified in an immunostained slice from the same animal (Fig.3D1, Table 2). These data are included in the group immunohistochemical analysis of cholinergic fiber density in NbM lesioned animals with intact ganglia (Fig. 1 D-F, Table 2). LFS LTD was successfully induced

in slices from all animals in this group and the magnitude of the LTD was not different from that observed in slices from sham lesioned animals (Figs. 3B3 and 3D3, sham NbM lesion: 78 +/- 2% of baseline fPSP, n=11 slices/ 7 animals vs NbM lesion + intact ganglia: 72+/- 2% of baseline fPSP, n=7 slices/ 6 animals, p>0.05; unpaired Student's *t* test).

Collectively, the immunohistochemical and electrophysiological data are consistent with the interpretation that a critical amount of cholinergic innervation is necessary to preserve function of mAChRs required for induction of both mLTD and LFS LTD at synapses in visual cortex. To further evaluate the relationship between the density of cholinergic innervation and the ability of synapses to express mAChR dependent LTD, we plotted the magnitude of mLTD or LFS LTD (expressed as % of baseline fPSP amplitude) versus the total cholinergic fiber length. It is important to note that we used only data in which the immunohistochemical staining and electrophysiological recording were obtained from the same slice (Fig. 4: mLTD; R value = 0.54, p=0.05: LFS LTD; R value = 0.57, p=0.07). As shown, the data from each experimental group are clustered, revealing a clear relationship between the presence (or absence) of mLTD or LFS LTD with the total cholinergic fiber length, promoting the idea that a threshold level of cholinergic innervation is required for induction of LTD.

Loss of plasticity is specific for visual cortex mLTD and LFS LTD

To ensure that the loss of mLTD and LFS LTD is specific to cholinergic dependent plasticities rather than a general loss of plasticity at layer 2/3 synapses, we tested whether a form of LTD induced by activation of α1 adrenergic receptors (NE LTD) is intact. We found that the magnitude of NE LTD induced by a 10 minute application of phenylephrine (100 μM, α1 specific agonist) is not different between groups (Fig 5A1-3, sham NbM lesion: 78 +/- 2% of baseline fPSP, n=4 slices/ 3 animals; NbM lesion + ganglionectomy:70 +/- 9% of fPSP baseline, n=5 slices/ 5 animals; NbM lesion + intact ganglia: 67 +/- 10% of fPSP baseline, n=5 slices/ 5 animals, p>0.05; ANOVA). Since m1 muscarinic and α1 adrenergic receptors both couple to Gαq, and both mLTD and NE LTD require the same signaling pathway for their induction (Scheiderer et al., 2008), this finding indicates that there is not a deficit in the downstream Gαq signaling pathway, but rather a specific loss of m1 receptor signaling.

We next wanted to confirm that the impact of NbM lesion with and without ganglionectomy is selective for synapses in visual cortex. Because cholinergic innervation of hippocampus originates in medial septum, mLTD at CA3-CA1 synapses should be completely unaffected by NbM lesion and ganglionectomy. As expected, the mLTD magnitude at CA3-CA1 synapses is indistinguishable in all lesion groups (Fig. 5B1-3, sham NbM lesion: 80 +/- 1% of baseline fPSP, n=4 slices/ 3 animals; NbM + ganglionectomy: 81 +/- 2 of baseline fPSP, n=6 slices/ 6 animals; NbM lesion + intact ganglia: 82 +/- 2% of baseline fPSP, n=5 slices/ 5 animals, p>0.05; ANOVA), indicating that cholinergic innervation to hippocampus is unaffected by our lesions.

mLTD in animals with sympathetic sprouting requires m3 but not m1 mAChRs

We recently reported that mLTD at layer 2/3 synapses requires extracellular signal regulated kinase (ERK) activation downstream of m1 mAChR activation, similar to hippocampus (Scheiderer et al., 2006, McCoy and McMahon, 2007, Volk et al., 2007). Furthermore, we find mLTD induction in young animals is unaffected by the m3 mAChR selective inhibitor 4-DAMP (100 nM, data not shown, 78 +/- 3% of baseline fPSP in 4-DAMP, n=5 slices/ 4 animals, vs 80 +/- 7% of baseline fPSP in interleaved controls without 4-DAMP, n=5 slices/ 4 animals, p>0.05; unpaired Student's *t* test). Therefore, we were interested to determine whether the “rescued” mLTD in animals with NbM lesion and intact ganglia remain dependent upon m1 receptors and ERK activation. We confirmed the presence of mLTD in sham lesioned and NbM lesioned animals with intact ganglia and examined the role of m1 mAChRs, m3 mAChRs, and ERK activation in each animal (all experiments were done interleaved in each animal

examined). In contrast to young rats, we found that in adult sham lesioned animals, inhibition of either m1 or m3 receptors blocks induction of mLTD, indicating a developmental change in the mAChRs required to induce the plasticity. As shown, bath application of pirenzepine (75nM, m1 selective antagonist) or 4-DAMP (100 nM, m3 selective antagonist) prevented mLTD (Figs 6A1, B1, 80 +/- 4% of baseline fPSP in sham NbM lesion without inhibitor (control), n=5 slices/ 4 animals, 102 +/- 2% of baseline fPSP in pirenzepine, n=4 slices/ 4 animals; 99 +/- 7% of baseline fPSP in 4-DAMP, n=4 slices/ 4 animals, $p<0.001$ compared to control; ANOVA). Interestingly, mLTD in animals with NbM lesion and intact ganglia was only prevented by 4-DAMP, while pirenzepine was without effect, suggesting that that m1 mAChRs are no longer required for induction of the plasticity (Fig. 6A2, B2, 82 +/- 9% of baseline fPSP in NbM lesion with intact ganglia without inhibitor (control), n=5 slices/ 5 animals; 82 +/- 7% of baseline fPSP in pirenzepine, n=5 slices/ 5 animals; 104 +/- 6% of baseline fPSP in 4-DAMP, n=5 slices/ 5 animals, $p<0.001$ compared to control; ANOVA).

Because both m1 and m3 mAChRs couple to Gαq, it remains possible that the “rescued” mLTD and the mLTD in sham NbM lesioned animals utilize the same downstream signaling molecules. We tested this and found that mLTD in both animal groups require activation of ERK, as both are inhibited by blocking ERK activation with U0126 (20 μM; Fig 6C1, C2, 102 +/-7% of baseline fPSP in U0126, n=5 slices/ 5 animals, $p<0.01$; paired Student's *t* test; 102 +/- 9% of baseline fPSP in U0126, n=5 slices/ 5 animals, $p<0.01$; paired Student's *t* test). This indicates that although it appears that different mAChR subtypes are required for inducing mLTD at synapses in sham versus NbM lesioned animals with intact ganglia, the same signaling molecule is required for mLTD in both animal groups.

Discussion

Our findings show that the repair mechanism we recently reported in hippocampus (Scheiderer et al., 2006) which is dependent upon sprouting from the autonomic nervous system is most likely a general mechanism that occurs in other brain regions impacted by cholinergic degeneration. Here we report that lesion of the NbM stimulates sprouting of adrenergic sympathetic fibers in visual cortex originating from the SCG that is accompanied by an increase in cholinergic innervation and the rescue/preservation of expression of two forms of LTD dependent upon mAChRs. When the SCG are removed bilaterally in animals with NbM lesion, both the increase in cholinergic innervation and the ability of synapses to express mLTD and LFS LTD are absent. These data demonstrate that sprouting from the SCG is required for the increased cholinergic innervation and the rescue/preservation of the mAChR dependent plasticities. It is important to mention that while the presence of mLTD and LFS LTD are correlated with both adrenergic and cholinergic sprouting, it seems most likely that the increased cholinergic innervation (rather than the adrenergic sprouting) is responsible for preserving/maintaining mLTD and LFS LTD since both plasticities require normal mAChR function for their induction.

Unfortunately, our data does not allow us to make a clear distinction between a “rescue” or “preservation” of the mAChR-dependent plasticities in animals with sympathetic sprouting. In our previous study in hippocampus, we reported that by 10 days post lesion, mLTD was absent in slices from animals with medial septal lesion and bilateral ganglionectomy, but was normal in lesioned animals with intact ganglia to permit sprouting. In experiments at 3 days post lesion, cholinergic degeneration was not yet complete and mLTD was normal in slices from both medial septal lesioned groups (Scheiderer et al., 2006). Collectively, these time course studies suggest that somewhere between 3 and 10 days post lesion, the mLTD is lost and subsequently rescued in lesioned animals with sympathetic sprouting. Alternatively, mLTD could be preserved or maintained if there is sufficient temporal overlap between cholinergic fiber degeneration and the onset of sympathetic sprouting. Thus, to distinguish

between a “rescue” or “preservation” of LTD by sympathetic sprouting, experiments are needed at daily intervals post lesion. However, high animal to animal variability in the timing of cholinergic degeneration and ingrowth of sympathetic sprouting at these early time points will likely make this issue difficult to resolve.

The source of the cholinergic fibers that are increased in animals with sympathetic sprouting is not known at this time. However, these fibers could originate from the SCG, as 1% of cells in this ganglion are cholinergic (Schafer et al., 1998). Alternatively, these fibers could arise from cholinergic cells endogenous to cortex or from cholinergic neurons in substantia innominata and globus pallidus which are known to innervate visual cortex (Houser et al., 1983, Eckenstein and Baughman, 1984). Finally, the increased cholinergic innervation could be a consequence of an adrenergic to cholinergic phenotype switch, as sympathetic neurons possess the ability to change their neurotransmitter identity (Furshpan et al., 1976, Wolinsky and Patterson, 1983, Francis and Landis, 1999, Weihe et al., 2005). Regardless of their origin, the increase in cholinergic innervation observed is dependent upon sprouting of adrenergic sympathetic fibers from the SCG. Detailed studies beyond the scope of the current study will be needed to resolve the precise origin of this sympathetic sprouting dependent increase in cholinergic innervation.

Cholinergic innervation, mAChR subtypes, and LTD

The ability of synapses in visual cortex to express mLTD and LFS LTD is correlated with the density of cholinergic fibers (Fig. 4). Cholinergic innervation in visual cortex in animals with NbM lesion and bilateral ganglionectomy is not completely absent because the NbM is not the only source of cholinergic input in this brain region (Houser et al., 1983,Eckenstein and Baughman, 1984). However, this remaining innervation is not sufficient to maintain the ability of synapses to express mLTD or LFS LTD. When the SCG remain intact, there is an approximate doubling of the number of VAChT positive fibers in visual cortex compared to animals with bilateral ganglionectomy, although the density of VAChT positive fibers is still severely decreased (approximately 35% of control) compared to that in sham NbM lesioned animals. Importantly, this relatively modest increase in cholinergic innervation in animals with intact ganglia and sympathetic sprouting is apparently enough to rescue or preserve both forms of LTD. These findings indicate that there is some threshold level of cholinergic activity required to ensure that the mechanisms necessary to induce LTD are available and function. Furthermore, our findings suggest this threshold lies in between the density of innervation in NbM lesioned animals with and without intact ganglia to permit sympathetic sprouting. Consideration must be given to the possibility that the VAChT positive fibers that remain following lesion and/or the m1 and m3 mAChRs present in visual cortex in the NbM lesioned animals with bilateral ganglionectomy do not function properly. The location of the remaining VAChT positive axons may be such that they are not in close enough proximity to the activated synapses in layer 2/3, or that there is not sufficient release of ACh in vivo to keep m1/m3 mAChRs adequately coupled to their signaling pathway to permit induction of either mLTD or LFS LTD. This potential loss of efficient mAChR-coupling to downstream signaling cascades as an explanation for the absence of cholinergic dependent LTD is supported by the reported decrease in CCh stimulated PI turnover that occurs following cholinergic degeneration in both humans with AD and animal models (Pearce and Potter, 1991, Ferrari-DiLeo and Flynn, 1993,Ferrari-DiLeo et al., 1995,Kolasa et al., 1997). The effectiveness of m1/m3 coupling to ERK activation in NbM lesioned animals with and without sympathetic sprouting will certainly be pursued in a future study.

mLTD at synapses in layer 2/3 in visual cortex of 3-4 week old animals requires activation of m1 mAChRs receptors (Kirkwood et al., 1999, Scheiderer et al., 2006, McCoy and McMahon, 2007). Here we report that while pharmacologically blocking m3 receptors with 4-DAMP has

no effect on mLTD induction in young animals, we find that inhibition of either m1 receptors with pirenzepine or m3 receptors with 4-DAMP prevents induction of mLTD in adult animals. This finding implies that during development, there is a recruitment of m3 mAChRs which participate in mLTD induction. Surprisingly, induction of mLTD in animals with NbM lesion and intact ganglia seems to only require m3 receptors (Fig. 6). However, mLTD induction in both sham NbM lesioned animals and in NbM lesioned animals with intact ganglia requires ERK activation, similarly to mLTD induction in young animals (Scheiderer et al., 2006, McCoy and McMahon, 2007, Volk et al., 2007). The apparent reliance of mLTD induction on only m3 receptors in animals with sympathetic sprouting is interesting and is a further demonstration of the brain's ability to adapt in an attempt to maintain normal function. It will be important to determine whether a requirement for m1 receptors is completely replaced by m3 receptors during the aging process in normal animals, as it is in the NbM lesioned animals. Previously, we have shown in the monocular region of adult tree shrew visual cortex that m3 rather than m1 receptors are entirely responsible for mLTD induction via an ERK signaling cascade (McCoy et al., 2008). Therefore, it is not surprising that a role for m3 receptors in mLTD induction is recruited and that mLTD in NbM lesioned animals with intact ganglia seems to only require m3 receptors for induction. Furthermore, since both m1 and m3 receptors couple to the same downstream signaling pathways including activation of ERK, the ability of these receptors to substitute for one another ensures the ability of synapses to undergo mLTD throughout development and during pathological states such as cholinergic degeneration.

Our finding that atropine completely blocks LFS LTD at layer 2/3 synapses is consistent with that of Origlia and coworkers (Origlia et al., 2006), who also showed that LFS LTD is absent in m1/m3 knockout mice (Origlia et al., 2006). However, these findings are in contrast to an elegant study by Choi et al., 2005 who showed that LFS LTD at layer 2/3 synapses can only be prevented by simultaneously blocking α1 adrenergic receptors, group I metabotropic glutamate receptors, and muscarinic m1 receptors, indicating a functional cooperation between these similarly coupled GPCRs (Choi et al., 2005). The discrepancies between the results are not clear, but could be related to differences in animal strains used, age of the animals at the time of experimentation, and/or recording conditions. In support of the findings by Choi et al., a similar cooperation between Gαq coupled receptors has been shown recently in another elegant set of studies at CA3-CA1 synapses (Volk et al., 2007), where m1 receptors and group I mGluRs cooperate in the induction of LFS LTD (Volk et al., 2007). We have also shown that in hippocampus, simultaneous weak activation of m1 mAChRs and α1 adrenergic receptors cooperate to induce an NMDAR-dependent form of LTD (Scheiderer et al., 2008).

Regarding the role of cholinergic innervation to visual cortex and the ability of synapses to express LTD, in the study by Choi et al., 2005, consistent with their pharmacological findings that multiple Gαq receptors cooperate to induce LTD, lesion of the NbM had no effect on induction of LFS LTD (Choi et al., 2005). However, in our experiments, LFS LTD was completely absent in animals with NbM lesion, consistent with our finding that atropine completely blocks LFS LTD. The reasons for these discrepancies are unknown. However a possible explanation is the compensatory role of sympathetic sprouting, which was not taken into consideration in the studies by Choi et al., although their experiments were performed before sprouting is likely to be robust. The present study suggests that a threshold level of cholinergic innervation is necessary to maintain or preserve the mechanisms required for induction of mLTD. Unfortunately, because the lesion conditions and the analysis of cholinergic fiber density were performed differently between the two studies, the discrepancies in the results cannot be easily resolved at this time.

Other studies examining the role of NbM lesions on visual cortical function with regard to expression of long-term plasticity and learning and memory suggest that while ACh may be important for these tasks, there are additional players at work. Specifically, following NbM

lesion, a theta burst stimulation protocol used to induce long-term potentiation in control animals instead induces LTD in lesioned animals (Kuczewski et al., 2005). Interestingly, following NbM lesion in both rats and macaque monkeys there is a period of impaired memory performance followed by recovery to control levels (Aigner et al., 1991, Balducci et al., 2003). This impairment and recovery may correlate with cholinergic denervation and subsequent sympathetic sprouting, further supporting a beneficial role for sympathetic sprouting.

Cholinergic dysfunction and memory

In AD, cognitive decline follows a pattern where an initial deficit is followed by a rebound in cognitive function, ending with a severe decline and permanent impairment (Gwyther, 2001). This rebound in cognitive function may be a consequence of the documented increase in cholinergic activity observed in early AD (Masliah et al., 1991, DeKosky et al., 2002, Frolich, 2002, Masliah et al., 2003, Mufson et al., 2003, Mufson et al., 2008). Thus, the increase in cholinergic innervation that occurs as a result of adrenergic sympathetic sprouting we have observed (Scheiderer et al., 2006 and current report) could be responsible for this increase in cholinergic function observed in humans. In fact, it may be the unidentified “abberant sprouting” that some suggest is responsible for the increased cholinergic function (Hashimoto and Masliah, 2003, Masliah et al., 2003). Because our data show a rescue/preservation of cholinergic dependent synaptic plasticity in animals with lesion of the medial septum (Scheiderer et al., 2006) or NbM (current report) when adrenergic sympathetic sprouting and the accompanying increase in cholinergic innervation is permitted, we speculate that learning and memory deficits will be less severe in these animals compared to animals without this compensatory sprouting. Accordingly, this sprouting could be the reason that some studies only observe a slight deficit in learning in various behavioral paradigms following cholinergic lesions (see Parent and Baxter, 2004; Fletcher et al., 2007, Gibbs and Johnson, 2007). Clearly future studies are needed to determine if animals with cholinergic lesion and intact SCG to permit sympathetic sprouting perform significantly better in learning assays compared to lesioned animals with bilateral ganglionectomy when sprouting is not possible. Finally, we speculate that at later stages, where there is massive cell loss and dramatic cognitive decline, these potential compensatory mechanisms dependent upon sympathetic sprouting are overwhelmed and no longer are capable of providing benefit. Indeed, further understanding of the role of sympathetic sprouting and its potential benefits to both hippocampal and cortical function could inform the development of more effective treatment regimens, to minimize cognitive decline and bolster this natural repair mechanism.

Supplementary Material

Refer to Web version on PubMed Central for supplementary material.

Acknowledgments

We thank Drs. Lindy Harrell and Krystyna Kolasa, as well as Umair Khan for technical assistance with nucleus basalis lesion and ganglionectomy surgeries. We also thank the Center for Glial Biology in Medicine Core.

Funding: This work was supported by the National Institute of Aging [AG21612 to L.L.M., NS57098]; National Eye Institute [T32 EY007033]; and the National Institute of Neurological Disorders and Stroke [F31 NS56835 to P.A.M.] and the NIH Neuroscience Blueprint Core Grant NS57098.

References

Aigner TG, Mitchell SJ, Aggleton JP, DeLong MR, Struble RG, Price DL, Wenk GL, Pettigrew KD, Mishkin M. Transient impairment of recognition memory following ibotenic-acid lesions of the basal forebrain in macaques. Exp Brain Res 1991;86:18–26. [PubMed: 1756788]

Balducci C, Nurra M, Pietropoli A, Samanin R, Carli M. Reversal of visual attention dysfunction after AMPA lesions of the nucleus basalis magnocellularis (NBM) by the cholinesterase inhibitor donepezil and by a 5-HT1A receptor antagonist WAY 100635. Psychopharmacology (Berl) 2003;167:28–36. [PubMed: 12618916]

Barefoot HC, Baker HF, Ridley RM. Synergistic effects of unilateral immunolesions of the cholinergic projections from the basal forebrain and contralateral ablations of the inferotemporal cortex and hippocampus in monkeys. Neuroscience 2000;98:243–251. [PubMed: 10854755]

Barefoot HC, Baker HF, Ridley RM. Crossed unilateral lesions of temporal lobe structures and cholinergic cell bodies impair visual conditional and object discrimination learning in monkeys. Eur J Neurosci 2002;15:507–516. [PubMed: 11876778]

Bentley P, Husain M, Dolan RJ. Effects of cholinergic enhancement on visual stimulation, spatial attention, and spatial working memory. Neuron 2004;41:969–982. [PubMed: 15046728]

Bierer LM, Haroutunian V, Gabriel S, Knott PJ, Carlin LS, Purohit DP, Perl DP, Schmeidler J, Kanof P, Davis KL. Neurochemical correlates of dementia severity in Alzheimer's disease: relative importance of the cholinergic deficits. J Neurochem 1995;64:749–760. [PubMed: 7830069]

Bodick NC, Offen WW, Shannon HE, Satterwhite J, Lucas R, van Lier R, Paul SM. The selective muscarinic agonist xanomeline improves both the cognitive deficits and behavioral symptoms of Alzheimer disease. Alzheimer Dis Assoc Disord 1997;11 4:S16–22. [PubMed: 9339268]

Booze RM, Mactutus CF, Gutman CR, Davis JN. Frequency analysis of catecholamine axonal morphology in human brain. II. Alzheimer's disease and hippocampal sympathetic ingrowth. J Neurol Sci 1993;119:110–118. [PubMed: 7902423]

Caccamo A, Fisher A, LaFerla FM. M1 agonists as a potential disease-modifying therapy for Alzheimer's disease. Curr Alzheimer Res 2009;6:112–117. [PubMed: 19355845]

Choi SY, Chang J, Jiang B, Seol GH, Min SS, Han JS, Shin HS, Gallagher M, Kirkwood A. Multiple receptors coupled to phospholipase C gate long-term depression in visual cortex. J Neurosci 2005;25:11433–11443. [PubMed: 16339037]

Clader JW, Wang Y. Muscarinic receptor agonists and antagonists in the treatment of Alzheimer's disease. Curr Pharm Des 2005;11:3353–3361. [PubMed: 16250841]

Conner JM, Varon S. Nerve growth factor influences the distribution of sympathetic sprouting into the hippocampal formation by implanted superior cervical ganglia. Exp Neurol 1994;130:15–23. [PubMed: 7821390]

Conner JM, Varon S. Effects of exogenous nerve growth factor upon sympathetic sprouting into the hippocampal formation. Exp Neurol 1995;136:123–135. [PubMed: 7498402]

Crutcher KA. Cholinergic denervation of rat neocortex results in sympathetic innervation. Exp Neurol 1981;74:324–329. [PubMed: 7286124]

Crutcher KA. Sympathetic sprouting in the central nervous system: a model for studies of axonal growth in the mature mammalian brain. Brain Res 1987;434:203–233. [PubMed: 3555709]

Davies P, Maloney AJ. Selective loss of central cholinergic neurons in Alzheimer's disease. Lancet 1976;2:1403. [PubMed: 63862]

Dechant G, Barde YA. The neurotrophin receptor p75(NTR): novel functions and implications for diseases of the nervous system. Nat Neurosci 2002;5:1131–1136. [PubMed: 12404007]

DeKosky ST, Ikonomovic MD, Styren SD, Beckett L, Wisniewski S, Bennett DA, Cochran EJ, Kordower JH, Mufson EJ. Upregulation of choline acetyltransferase activity in hippocampus and frontal cortex of elderly subjects with mild cognitive impairment. Ann Neurol 2002;51:145–155. [PubMed: 11835370]

Dobrunz LE, Stevens CF. Heterogeneity of release probability, facilitation, and depletion at central synapses. Neuron 1997;18:995–1008. [PubMed: 9208866]

Drachman DA, Leavitt J. Human memory and the cholinergic system. A relationship to aging? Arch Neurol 1974;30:113–121. [PubMed: 4359364]

Dudek SM, Bear MF. Bidirectional long-term modification of synaptic effectiveness in the adult and immature hippocampus. J Neurosci 1993;13:2910–2918. [PubMed: 8331379]

Dunnett SB, Fibiger HC. Role of forebrain cholinergic systems in learning and memory: relevance to the cognitive deficits of aging and Alzheimer's dementia. Prog Brain Res 1993;98:413–420. [PubMed: 8248529]

Eckenstein F, Baughman RW. Two types of cholinergic innervation in cortex, one co-localized with vasoactive intestinal polypeptide. Nature 1984;309:153–155. [PubMed: 6717593]

Ferrari-DiLeo G, Flynn DD. Diminished muscarinic receptor-stimulated [3H]-PIP2 hydrolysis in Alzheimer's disease. Life Sci 1993;53:PL439–444. [PubMed: 8255145]

Ferrari-DiLeo G, Mash DC, Flynn DD. Attenuation of muscarinic receptor-G-protein interaction in Alzheimer disease. Mol Chem Neuropathol 1995;24:69–91. [PubMed: 7755848]

Fisher A. Cholinergic treatments with emphasis on m1 muscarinic agonists as potential disease-modifying agents for Alzheimer's disease. Neurotherapeutics 2008;5:433–442. [PubMed: 18625455]

Fisher A, Michaelson DM, Brandeis R, Haring R, Chapman S, Pittel Z. M1 muscarinic agonists as potential disease-modifying agents in Alzheimer's disease. Rationale and perspectives. Ann N Y Acad Sci 2000;920:315–320. [PubMed: 11193170]

Fletcher BR, Baxter MG, Guzowski JF, Shapiro ML, Rapp PR. Selective cholinergic depletion of the hippocampus spares both behaviorally induced Arc transcription and spatial learning and memory. Hippocampus 2007;17:227–234. [PubMed: 17286278]

Francis NJ, Landis SC. Cellular and molecular determinants of sympathetic neuron development. Annu Rev Neurosci 1999;22:541–566. [PubMed: 10202548]

Frolich L. The cholinergic pathology in Alzheimer's disease--discrepancies between clinical experience and pathophysiological findings. J Neural Transm 2002;109:1003–1013. [PubMed: 12111437]

Furshpan EJ, MacLeish PR, O'Lague PH, Potter DD. Chemical transmission between rat sympathetic neurons and cardiac myocytes developing in microcultures: evidence for cholinergic, adrenergic, and dual-function neurons. Proc Natl Acad Sci U S A 1976;73:4225–4229. [PubMed: 186792]

Gibbs RB, Johnson DA. Cholinergic lesions produce task-selective effects on delayed matching to position and configural association learning related to response pattern and strategy. Neurobiol Learn Mem 2007;88:19–32. [PubMed: 17449284]

Gwyther, LP. Caring for People with Alzheimer's Disease: A Manual for Facility Staff. Washington D.C.: American Health Care Association; 2001.

Harrell LE, Kolasa K, Parsons DS, Ayyagari V. Hippocampal sympathetic ingrowth and cholinergic denervation uniquely alter muscarinic receptor subtypes in the hippocampus. Brain Res 1995;676:386–393. [PubMed: 7614010]

Hashimoto M, Masliah E. Cycles of aberrant synaptic sprouting and neurodegeneration in Alzheimer's and dementia with Lewy bodies. Neurochem Res 2003;28:1743–1756. [PubMed: 14584828]

Houser CR, Crawford GD, Barber RP, Salvaterra PM, Vaughn JE. Organization and morphological characteristics of cholinergic neurons: an immunocytochemical study with a monoclonal antibody to choline acetyltransferase. Brain Res 1983;266:97–119. [PubMed: 6850348]

Kirkwood A, Rozas C, Kirkwood J, Perez F, Bear MF. Modulation of long-term synaptic depression in visual cortex by acetylcholine and norepinephrine. J Neurosci 1999;19:1599–1609. [PubMed: 10024347]

Kolasa K, Harrell LE, Parsons DS. Effect of hippocampal sympathetic ingrowth and cholinergic denervation on hippocampal phospholipase C activity and G-protein function. Neuroscience 1997;77:111–120. [PubMed: 9044379]

Kuczewski N, Aztiria E, Leanza G, Domenici L. Selective cholinergic immunolesioning affects synaptic plasticity in developing visual cortex. Eur J Neurosci 2005;21:1807–1814. [PubMed: 15869476]

Loy R, Moore RY. Anomalous innervation of the hippocampal formation by peripheral sympathetic axons following mechanical injury. Exp Neurol 1977;57:645–650. [PubMed: 908390]

Masliah E, Alford M, Adame A, Rockenstein E, Galasko D, Salmon D, Hansen LA, Thal LJ. Abeta1-42 promotes cholinergic sprouting in patients with AD and Lewy body variant of AD. Neurology 2003;61:206–211. [PubMed: 12874400]

Masliah E, Mallory M, Hansen L, Alford M, Albright T, DeTeresa R, Terry R, Baudier J, Saitoh T. Patterns of aberrant sprouting in Alzheimer's disease. Neuron 1991;6:729–739. [PubMed: 1827266]

Mayo W, Kharouby M, Le Moal M, Simon H. Memory disturbances following ibotenic acid injections in the nucleus basalis magnocellularis of the rat. Brain Res 1988;455:213–222. [PubMed: 3401780]

McCoy PA, McMahon LL. Muscarinic Receptor Dependent Long Term Depression in Rat Visual Cortex is PKC Independent but Requires ERK1/2 Activation and Protein Synthesis. J Neurophysiol 2007;98:1862–1870. [PubMed: 17634336]

McCoy PA, Norton TT, McMahon LL. Layer 2/3 synapses in monocular and binocular regions of tree shrew visual cortex express mAChR dependent long-term depression and long-term potentiation. J Neurophysiol. 2008

Mufson EJ, Counts SE, Perez SE, Ginsberg SD. Cholinergic system during the progression of Alzheimer's disease: therapeutic implications. Expert Rev Neurother 2008;8:1703–1718. [PubMed: 18986241]

Mufson EJ, Ginsberg SD, Ikonomovic MD, DeKosky ST. Human cholinergic basal forebrain: chemoanatomy and neurologic dysfunction. J Chem Neuroanat 2003;26:233–242. [PubMed: 14729126]

Nobili L, Sannita WG. Cholinergic modulation, visual function and Alzheimer's dementia. Vision Res 1997;37:3559–3571. [PubMed: 9425531]

Origlia N, Kuczewski N, Aztiria E, Gautam D, Wess J, Domenici L. Muscarinic acetylcholine receptor knock-out mice show distinct synaptic plasticity impairments in the visual cortex. J Physiol 2006;577:829–840. [PubMed: 17023506]

Parent MB, Baxter MG. Septohippocampal acetylcholine: involved in but not necessary for learning and memory? Learn Mem 2004;11:9–20. [PubMed: 14747512]

Pearce BD, Potter LT. Coupling of m1 muscarinic receptors to G protein in Alzheimer disease. Alzheimer Dis Assoc Disord 1991;5:163–172. [PubMed: 1772636]

Perry EK, Perry RH, Blessed G, Tomlinson BE. Changes in brain cholinesterases in senile dementia of Alzheimer type. Neuropathol Appl Neurobiol 1978;4:273–277. [PubMed: 703927]

Rizzo M, Anderson SW, Dawson J, Nawrot M. Vision and cognition in Alzheimer's disease. Neuropsychologia 2000;38:1157–1169. [PubMed: 10838150]

Scalapino K, Conner JM, Varon S. The role of NGF and afferent denervation in the process of sympathetic fiber ingrowth into the hippocampal formation. Exp Neurol 1996;141:310–317. [PubMed: 8812166]

Schafer MK, Eiden LE, Weihe E. Cholinergic neurons and terminal fields revealed by immunohistochemistry for the vesicular acetylcholine transporter. II. The peripheral nervous system. Neuroscience 1998;84:361–376. [PubMed: 9539210]

Scheiderer CL, McCutchen E, Thacker EE, Kolasa K, Ward MK, Parsons D, Harrell LE, Dobrunz LE, McMahon LL. Sympathetic sprouting drives hippocampal cholinergic reinnervation that prevents loss of a muscarinic receptor-dependent long-term depression at CA3-CA1 synapses. J Neurosci 2006;26:3745–3756. [PubMed: 16597728]

Scheiderer CL, Smith CC, McCutchen E, McCoy PA, Thacker EE, Kolasa K, Dobrunz LE, McMahon LL. Coactivation of M1 muscarinic and alpha1 adrenergic receptors stimulates extracellular signal-regulated protein kinase and induces long-term depression as ca3-ca1 synapses in rat hippocmapus. J Neurosci 2008;28:5350–5358. [PubMed: 18480291]

Volk LJ, Pfeiffer BE, Gibson JR, Huber KM. Multiple Gq-coupled receptors converge on a common protein synthesis-dependent long-term depression that is affected in fragile X syndrome mental retardation. J Neurosci 2007;27:11624–11634. [PubMed: 17959805]

Weihe E, Schutz B, Hartschuh W, Anlauf M, Schafer MK, Eiden LE. Coexpression of cholinergic and noradrenergic phenotypes in human and nonhuman autonomic nervous system. J Comp Neurol 2005;492:370–379. [PubMed: 16217790]

Whitehouse PJ, Price DL, Struble RG, Clark AW, Coyle JT, Delon MR. Alzheimer's disease and senile dementia: loss of neurons in the basal forebrain. Science 1982;215:1237–1239. [PubMed: 7058341]

Wolinsky E, Patterson PH. Tyrosine hydroxylase activity decreases with induction of cholinergic properties in cultured sympathetic neurons. J Neurosci 1983;3:1495–1500. [PubMed: 6134789]

Abbreviations

AD	Alzheimer's disease
aCSF	artificial cerebrospinal fluid
CCH	carbachol
ChAT	choline acetyl transferase
DAMP	1,1-Dimethyl-4-diphenylacetoxypiperidinium iodide

DMSO	Dimethyl sulfoxide
ERK	extracellular regulated kinase
fPSP	field post-synaptic potential
GPCR	g protein coupled receptor
LFS LTD	low frequency stimulation induced LTD
LTD	long-term depression
mAChR	muscarinic acetylcholine receptor
mGluR	metabotropic glutamate receptor
mLTD	muscarinic receptor dependent LTD
NbM	nucleus basalis magnocellularis
NDS	normal donkey serum
NE LTD	norepinephrine induced LTD
PBS	phosphate buffered saline
PFA	paraformaldehyde
PPR	paired pulse ratio
p75NTR	p75 neurotrophin receptor
SCG	superior cervical ganglia
TH	tyrosine hydroxylase
VAChT	vesicular acetylcholine transporter

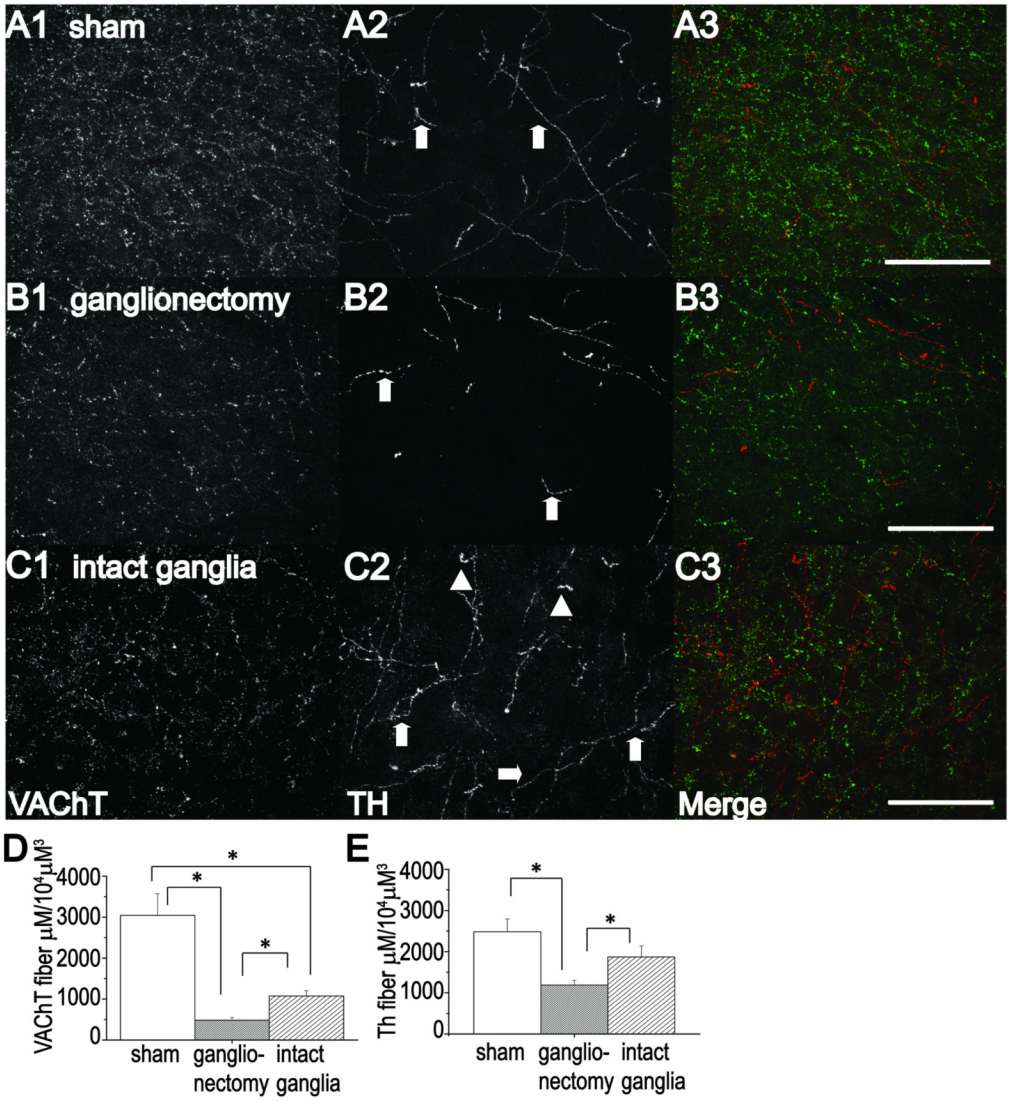

Figure 1.

An increase in cholinergic innervation accompanies adrenergic sympathetic sprouting in visual cortex. Analysis of sections stained using anti-VAChT immunohistochemistry **(A1-C1, A3-C3)** (to label cholinergic fibers: green fibers in **A3-C3**) and anti-TH immunohistochemistry **(A2-C2, A3-C3)** (to label adrenergic fibers; red fibers in **A3-C3**) shows more VAChT positive fibers in sham NbM lesioned animals **(A1,A3)** compared to animals with NbM lesion with ganglionectomy **(B1,B3)** or NbM lesion with intact ganglia**(C1,C3)**. Note the thick torturous TH positive fibers (**A2,C2,** arrowheads) indicative of sympathetic sprouting as compared to fine, delicate fibers (**A2-C2**, arrows) originating from locus coeruleus. Bar charts demonstrate a significant increase in total length of VAChT **(D)** and TH **(E)** positive fibers in NbM lesioned animals with intact ganglia compared to NbM lesioned animals with bilateral ganglionectomy, indicating presence of adrenergic sympathetic sprouting and the accompanying cholinergic reinnervation. Scale Bar, **A-C**; 100 µm.

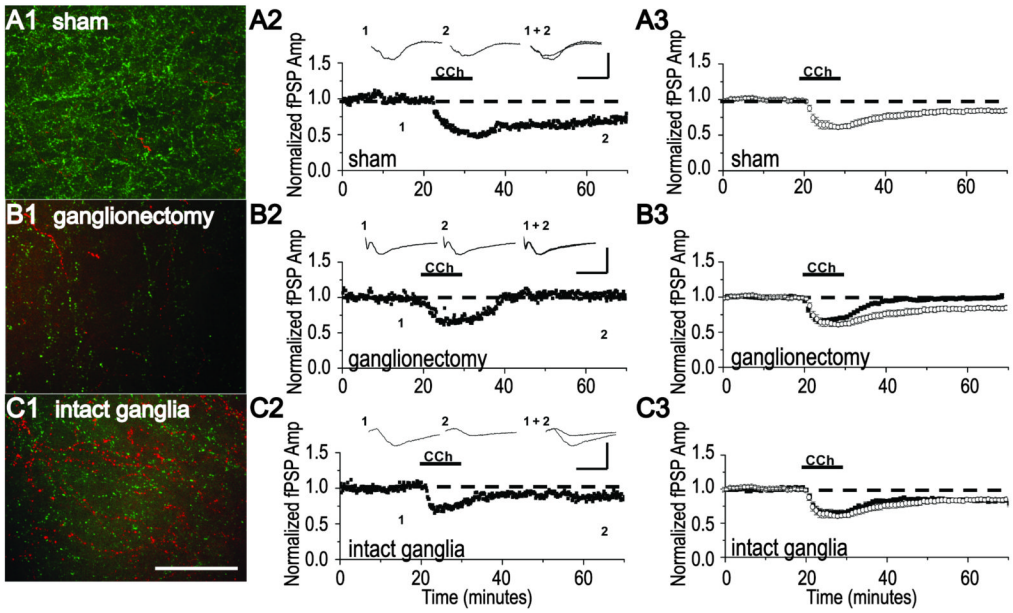

Figure 2.

mLTD is absent in NbM lesioned animals with bilateral ganglionectomy but is present in NbM lesioned animals with intact ganglia to permit sympathetic sprouting and a recovery of cholinergic innervation. **(A1)** Representative example of double anti-TH (red) and anti-VAChT (green) immunohistochemistry and **(A2)** a mLTD experiment at layer 2/3 synapses in an acute slice of visual cortex. Data were obtained in separate slices from the same sham NbM lesioned animal. **(A3)** Group electrophysiology data (open symbols) demonstrating mLTD is induced in slices from sham NbM lesioned animals. **(B1)** Representative example of double anti-TH (red) and anti-VAChT (green) immunohistochemistry and **(B2)** a mLTD experiment in the same slice from an NbM lesioned animal with bilateral ganglionectomy. **(B3)** Group electrophysiology data (filled symbols) demonstrating that mLTD is absent in slices from NbM lesioned animals with bilateral ganglionectomy. **(C1)** Representative example of double anti-TH (red) and anti-VAChT (green) immunohistochemistry and **(C2)** a mLTD experiment in the same slice from an NbM lesioned animal with intact ganglia. **(C3)** Group electrophysiology data (filled symbols) demonstrating mLTD is induced in slices from NbM lesioned animals with intact ganglia. Averaged mLTD data from sham lesioned animals shown in A3 (open symbols) is replotted in B3 and C3 to facilitate comparison (open symbols). Scale bar, **A1-C1**; 100 μm. Waveforms are averages of 20 events taken from 5 min before and 35 min after either CCh application. Scale bar, **A2-C2;** 0.5 mV, 10 ms.

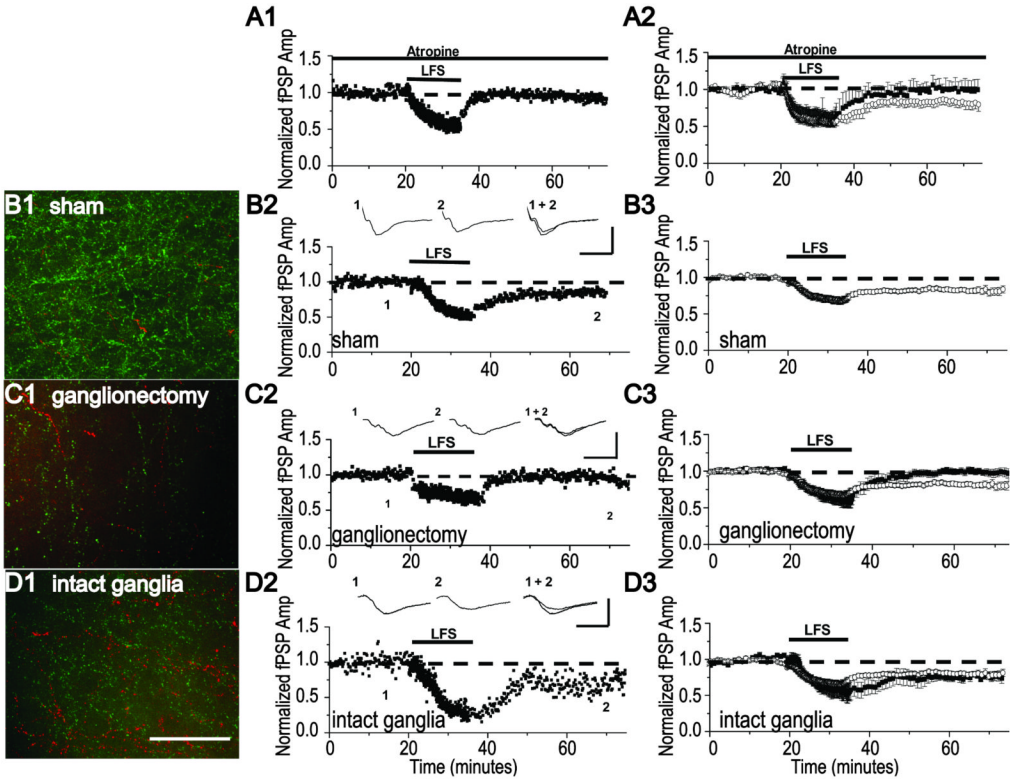

Figure 3.

LFS LTD is absent in NbM lesioned animals with bilateral ganglionectomy but is present in NbM lesioned animals with intact ganglia. **(A1)** Single example and **(A2)** group electrophysiology data (filled symbols) demonstrating that LFS LTD is prevented by 1μM atropine, a nonselective mAChR antagonist. **(B1)** Representative example of double anti-TH (red) and anti-VAChT (green) immunohistochemisty (image replotted from Fig. 2A1) and **(B2)** a LFS LTD experiment in separate slices from the same sham NbM lesioned animal as in Fig.2A. **(B3)** Group electrophysiology data (open symbols) demonstrating LFS LTD is induced in slices from sham NbM lesioned animals. **(C1)** Representative example of double anti-TH (red) and anti-VAChT (green) immunohistochemisty (image replotted from Fig. 2B1) and **(C2)** a LFS LTD experiment in separate slices from the same NbM lesioned animal with bilateral ganglionectomy as in Fig.2B. **(C3)** Group electrophysiology data (filled symbols) demonstrating LFS LTD is absent in slices from NbM lesioned animals with bilateral ganglionectomy. **(D1)** Representative example of double anti-TH (red) and anti-VAChT (green) immunohistochemisty and **(D2)** a LFS LTD experiment in separate slices from the same NbM lesioned animal with intact ganglia. **(D3)** Group electrophysiology data (filled symbols) demonstrating LFS LTD is induced in slices from NbM lesioned animals with intact ganglia. Averaged LFS LTD from sham NbM lesioned animals shown in B3 is replotted in A3, C3 and D3 to facilitate comparison (open symbols). Scale Bar, **B1-D1**; 100 μm. Waveforms are averages of 20 events taken from 5 min before and 35 min after either CCh application. Scale bar, **B2-D2;** 0.5 mV, 10 ms.

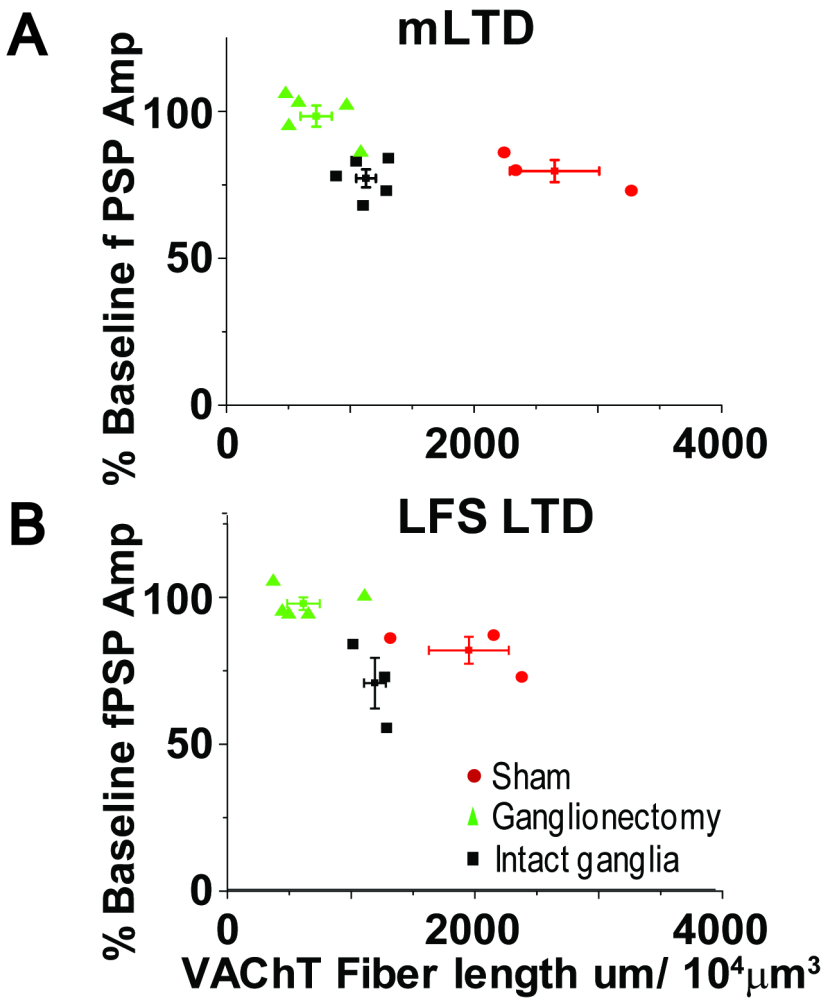

Figure 4.

LTD magnitude correlates with total VAChT staining. Total VAChT fiber length plotted versus magnitude of **(A)** mLTD and **(B)** LFS LTD. The immunohistochemistry and electrophysiology were obtained from the same slice. These data demonstrate a significant correlation between the amount of VAChT staining and the presence of LTD.

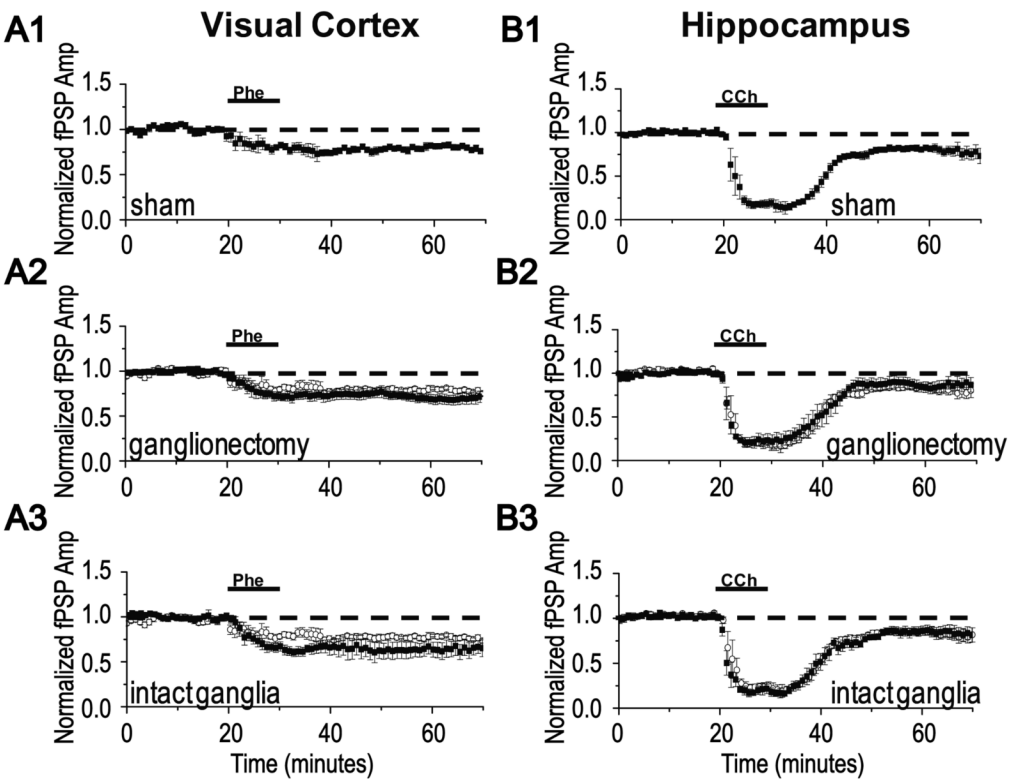

Figure 5.

NE LTD in visual cortex and mLTD in hippocampus are unaffected by NbM lesion with or without ganglionectomy. **(A)** LTD induced by α1 adrenergic receptor activation (NE LTD) using the selective agonist phenylephrine (100 μM) is not significantly different in magnitude in slices from animals with (**A1**) sham NbM lesion, (**A2**) NbM lesion with ganglionectomy (filled symbols), or (**A3**) NbM lesion with intact ganglia (filled symbols). Averaged NE LTD from sham NbM lesioned animals shown in A1 is replotted in A2 and A3 to facilitate comparison (open symbols). **(B)** mLTD at hippocampal CA3-CA1 synapses is not significantly different in magnitude in slices from animals with (**B1**) sham NbM lesion, (**B2**) NbM lesion with ganglionectomy (filled symbols), or (**B3**) NbM lesion with intact ganglia (filled symbols). Averaged hippocampal mLTD from sham NbM lesioned animals shown in B1 is replotted in B2 and B3 to facilitate comparison (open symbols).

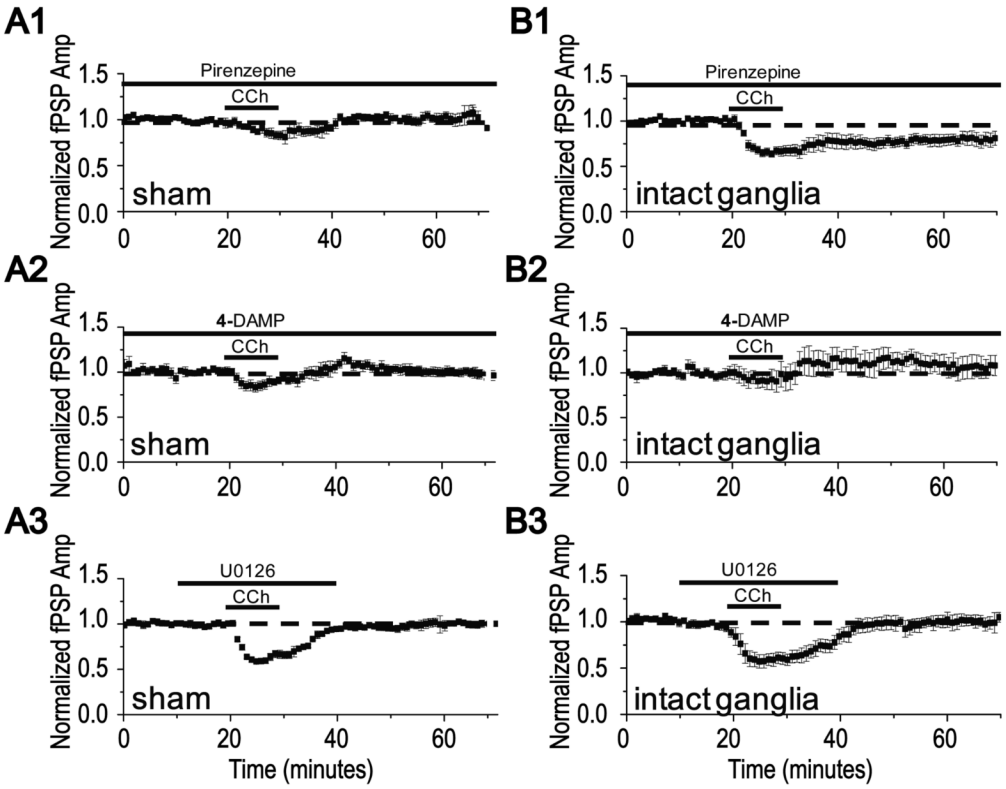

Figure 6.

Induction of mLTD in sham NbM lesioned animals and in NbM lesioned animals with intact ganglia requires activation of different mAChRs, but shares a requirement of ERK activation. **(A1,A2)** Blockade of m1 receptors by application of 75nM pirenzepine prevents mLTD in slices from sham NbM lesioned animals, but has no effect on mLTD in slices from NbM lesioned animals with intact ganglia. **(B1,B2)** mLTD induction is blocked by 100μM 4-DAMP, a m3 receptor antagonist, in slices from both sham NbM lesioned animals and NbM lesioned animals with intact ganglia. **(C1, C2)** mLTD induction is blocked by 20 μM U0126, an inhibitor of ERK activation, in slices from both sham NbM lesioned animals and NbM lesioned animals with intact ganglia.

Table 1

Analysis of anti-TH Immunohistochemistry Data are represented as +/- S.E.M. ** $p < 0.05$ when compared to sham lesion. ^{t} $p < 0.05$ when compared to NbM lesion with intact ganglia. $^{+}$ $p < 0.001$ when compared to NbM lesion with intact ganglia. ANOVA.

	Total TH Fiber Length (μM)	Mean Fiber Length (μM)	Total Number of Fibers
Sham Lesion	2064 +/- 366	43 +/- 4	45 +/- 6
NbM lesion with ganglionectomy	1516 +/- 217 ** ^{t}	53+/- 5	29 +/- 3 ** ^{t}
NbM lesion with intact ganglia	1826 +/- 293	55 +/- 5	35 +/- 5

Table 2

Analysis of anti-VAChT immunohistochemistry and corresponding LTD Data are represented as +/- S.E.M ** $p < 0.001$ when compared to sham Lesion. ^{t} $p < 0.05$ when compared to NbM lesion with intact ganglia. $^{+}$ $p < 0.001$ when compared to NbM lesion with intact ganglia; ANOVA.

	Total VAChT Fiber Length (μM)	Mean Fiber Length (μM)	Total Number of Fibers	% of baseline fPSP
sham lesion averaged data	3042 +/- 527	29 +/- 2	101 +/- 42	mLTD: 80 +/- 1 LFS LTD: 78 +/- 2
Representative examples from a single sham lesioned animal: Fig 2A/ 3B	3389	33 +/- 2	165	mLTD: 75 LFS LTD: 83
NbM lesion with ganglionectomy averaged data	484 +/- 70 ** ^{t}	25 +/- 1	20 +/- 3 ** $^{+}$	mLTD: 99 +/- 1 ** $^{+}$ LFS LTD: 97 +/- 2 ** $^{+}$
Representative examples from a single animal with NbM lesion with ganglionectomy: Fig 2B/ 3C	583	27 +/- 2	22	mLTD: 102 LFS LTD: 98
NbM with intact ganglia averaged data	1074 +/- 127 **	26 +/- 2	45 +/- 6 **	mLTD 81 +/- 1 LFS LTD 72+/- 2
Representative examples from a single animal with NbM lesion with intact ganglia: Fig 2C	1308	30 +/- 1	44	mLTD: 85
Representative examples from a single animal with NbM lesion with intact ganglia: Fig 3D	1292	29 +/- 1	45	LFS LTD: 74